

Endosialin-expressing pericytes promote metastatic dissemination

Carmen Viski^{1*}, Courtney König^{2,3*}, Magdalena Kijewska¹, Carolin Mogler^{2,4},
Clare M. Isacke^{1#}, and Hellmut G. Augustin^{2,3,5#}

¹The Breast Cancer Now Toby Robins Research Centre, The Institute of Cancer Research, London, United Kingdom; ²Division of Vascular Oncology and Metastasis (DKFZ-ZMBH Alliance), German Cancer Research Center, Heidelberg, Germany; ³Department of Vascular Biology and Tumor Angiogenesis (CBTM), Medical Faculty Mannheim, Heidelberg University; ⁴Institute of Pathology, Heidelberg University, Im Neuenheimer Feld 224, 69120 Heidelberg, Germany; ⁵German Cancer Consortium, Heidelberg, Germany.

Authorship note: *, # These authors contributed equally to this study.

Keywords: intravasation, metastasis, pericytes, stroma, endosialin.

Running title: Activated pericytes promote metastatic dissemination

Word count: manuscript: 6.108 words (excl. references); abstract: 148 words

CORRESPONDING AUTHORS

Professor Clare Isacke, The Breast Cancer Now Toby Robins Research Centre, The Institute of Cancer Research, 237 Fulham Road, London SW3 6JB, United Kingdom. Phone: 44-20-7153-5510; Fax: 44-20-7153-5340; Email: clare.isacke@icr.ac.uk

or

Professor Hellmut Augustin, Joint Research Division of Vascular Biology, Medical Faculty Mannheim (CBTM), Heidelberg University, and German Cancer Research Center Heidelberg (DKFZ-ZMBH Alliance), Im Neuenheimer Feld 280, D-69221 Heidelberg, Germany. Phone: 49-6221-421500; Fax: 49-6221-421515; Email: augustin@angiogenese.de

FINANCIAL SUPPORT

This work was funded by Breast Cancer Now (to C.M. Isacke), a Medical Research Council PhD studentship (to C. Viski), grants from the Deutsche Forschungsgemeinschaft (SFB-TR23 'Vascular Differentiation and Remodeling' [to H.G. Augustin]) and the Helmholtz Alliance 'Preclinical Comprehensive Cancer Center' [to H.G. Augustin]. C.M. Isacke acknowledges NHS funding to the NIHR Biomedical Research Centre at The Royal Marsden and the ICR. H.G. Augustin is supported by an endowed chair from the Aventis Foundation.

DISCLOSURE AND POTENTIAL CONFLICTS OF INTERESTS

The authors disclose no potential conflicts of interest.

ABSTRACT

Metastasis is a multistep process that is critically dependent on the interaction of metastasizing tumor cells with cells in the local microenvironment. Within this tumor stroma, vessel-associated pericytes and myofibroblasts share a number of traits including the upregulated expression of the transmembrane receptor endosialin (CD248). Comparative experiments in wildtype and endosialin-deficient mice revealed that stromal endosialin does not affect primary tumor growth but strongly promotes spontaneous metastasis. Mechanistically, endosialin-expressing pericytes in the primary tumor facilitate distant site metastasis by promoting tumor cell intravasation in a cell contact-dependent manner resulting in elevated numbers of circulating tumor cells. Corresponding to these preclinical experiments, in independent cohorts of primary human breast cancers, upregulated endosialin expression significantly correlates with increased metastasis and poorer patient survival. Together, the data demonstrate a critical role for endosialin-expressing primary tumor pericytes in mediating metastatic dissemination and identify endosialin as a promising therapeutic target in breast cancer.

INTRODUCTION

The vast majority of cancer-related mortality is due to distant site metastasis and not to primary tumor growth. Metastasis thereby marks the transition from a local to a systemic disease. The multistep nature of metastatic tumor cell dissemination and colonization is widely appreciated (1). Yet, the molecular and mechanistic understanding of individual steps of the metastatic cascade and the identification of bottlenecks that could serve as therapeutic targets is still in its infancy.

Metastatic progression is critically dependent on the interaction of metastasizing tumor cells with the cells of their microenvironment, both at the primary tumor site as well as at the site of metastasis (2,3). Among the cells of the tumor microenvironment, stromal myofibroblasts, macrophages and other inflammatory cells, as well as cellular constituents of blood and lymphatic vessels, i.e. endothelial cells, pericytes and vascular smooth muscle cells, comprise the tumor stroma (4,5). Interestingly, tumor-associated pericytes and stromal myofibroblasts share a number of functional and molecular traits including the expression of the cell surface receptor endosialin (CD248).

Endosialin (CD248) is a transmembrane glycoprotein (6) that was originally described as a cell surface marker of the tumor endothelium (7,8). However, high-resolution morphological analyses of a range of human cancers have unequivocally demonstrated that endosialin is not expressed by endothelial cells, but by pericytes and myofibroblasts (9-13). Importantly, resting mesenchymal cells in the healthy adult have low or undetectable levels of endosialin expression. Expression is essentially restricted to activated cells of the mesenchymal lineage during embryogenesis (10,14) as well as during pathological states including tumor progression and metastasis (13,15,16), making endosialin an oncofetal protein with potential as a biomarker and a therapeutic target (17-20). In fact, clinical trials in solid tumors and lymphomas with an endosialin targeting antibody are ongoing (www.clinicaltrials.gov/ct2/results?term=endosialin&Search=Search) (21).

Functionally, endosialin regulates mesenchymal cell proliferation through PDGFR β signaling (22,23), which has been associated with the promigratory mesenchymal cell phenotype (24-26). Endosialin-deficient mice are, unless pathologically challenged, phenotypically normal (27), although

they display some delay of developmental vascular remodeling caused by perturbed pericyte function (28, 29). Earlier studies have reported no overt difference in the growth of subcutaneous tumors in wildtype and endosialin-deficient mice (27,28,30). Yet, transplantable colorectal tumors grown orthotopically in endosialin-deficient mice, displayed a prominent reduction in primary tumor growth, invasion and metastasis compared to endosialin wildtype tumor-bearing mice (27). This striking difference between subcutaneous and orthotopic tumor growth in endosialin-deficient mice prototypically highlights the important contribution of the microenvironment to tumor progression and metastasis and identifies endosialin as a functionally relevant receptor in the tumor stroma. At the same time, pericytes have been shown to limit metastasis in the Rip1Tag2 model of pancreatic β cell tumorigenesis (31). Conceptually linking these two totally independent lines of research, we hypothesized that the upregulated expression of endosialin by tumor-associated pericytes may be an important contributor to tumor progression and metastasis. We consequently set out to systematically dissect the role of endosialin in the control of individual steps of the metastatic cascade. These experiments yielded unexpected mechanistic insights into the role of endosialin in regulating metastasis and identified the control of tumor cell intravasation by activated pericytes as a critical and rate-limiting step.

METHODS

In vivo studies

In vivo experiments were carried out under a UK Home Office Project license 70/7413 or under ethical guidelines of the local Animal Use and Care Committees approved by the Regierungspräsidium in Karlsruhe, Germany [35-9185.81/G-195/10]. Animals were housed in barriers at the animal facility of the DKFZ or in Optimice cages at the ICR. All animals were monitored on a daily basis for signs of ill health and had free admission to food and water. 129/Sv mice with a global knockout of endosialin were kindly provided by Dr. David Huso (Johns Hopkins Medical Institutions, Baltimore, USA) (27). Mice were backcrossed for 6 generations with either BALB/c (Charles River), Swiss nude mice (Charles River) or C57BL/6 (DKFZ) mice. Genotypes were confirmed by PCR.

For spontaneous metastasis assays, 4T1 tumor cells were injected into the mammary fat pad or subcutaneously in 6-10 weeks old female WT or EN^{KO} BALB/c or Swiss nude mice. LLC cells were implanted subcutaneously in the flank of 8-10 weeks old WT or EN^{KO} C57BL/6 mice. Tumor size was monitored by IVIS imaging. Tumor volume was calculated as $0.5 \times \text{length} \times \text{width}^2$.

For 4T1 or LLC tumor resection, primary tumors were removed under general anesthesia. Mice with tumors not effectively removed or with subsequent tumor recurrence were removed from analyses. Mice were sacrificed at the indicated time points or when they showed signs of ill health.

Protocols for tissue processing, vascular leakage and hypoxia assessment are described in the Supplementary Data.

***Ex vivo* culture of circulating tumor cells**

Arterial blood was isolated by cardiac puncture and 100 μ L plated in DMEM plus 10% FCS per 10cm tissue culture plate. Tumor cell colonies were stained 14 days later with crystal violet. Plates were scanned at 300dpi on EpsonV700 scanner and analyzed by Adobe Photoshop CS6.

Cells

4T1 cells (ATCC, 2013), 4T1 cells expressing luciferase (4T1-Luc; provided by Dr. K. Srivastava, DKFZ, 2014), 4T1 or 4T1-Luc cells expressing RFP (4T1-RFP, 4T1-Luc-RFP) were cultured in DMEM or RPMI (Invitrogen) plus 10% FCS (Invitrogen). Lewis lung carcinoma cells (LLC; obtained from ATCC, 2006) were cultured in DMEM supplemented with 10% FCS, 1% penicillin/streptomycin. Human MDA-MB-231-LM2 expressing luciferase and GFP (MDA-MB213-Luc-GFP; provided by Dr. C. Lowry, DKFZ, 2014) cells were cultured in DMEM plus 10% FCS, 1% penicillin/streptomycin. Cell authentication by Multiplexion GmbH resulted in 98% identity towards MDA-MB-231 cells (Dec. 2015).

Human umbilical vein endothelial cells (HUVEC, Nov. 2015, tested by Promocell via flow cytometry and PCR) were cultured in Endopan3 medium with supplements (PAN, Biotech GmbH). The immortalized mouse endothelial cell line sEND (provided by R. Bicknell, University of Birmingham) was cultured in DMEM plus 10% fetal calf serum. Human brain vascular pericytes (BP, Nov. 2015, tested by ScienCell via immunofluorescence and PCR) and 10T1/2 cells (ATCC, 1997) were cultured in pericyte medium (ScienCell) plus 2% FCS, 1% of the corresponding pericyte growth supplement (PGS) and 1% penicillin/streptomycin, according to manufacturer's protocol. BP were infected with pGIPZ lentiviral vectors (Dharmacon) containing control (shNT, GIPZ shRNA Empty Vector; RHS4349) or endosialin-targeting (shEN: V2LHS_34217) shRNAs at a multiplicity of infection (MOI) of 10. 10T1/2 cells were infected with MISSION shRNA lentivirus particles (Sigma) encoding non-targeting (SHC002V) endosialin targeting (shEN; TRC0000098115) shRNAs at a MOI of 5. Cells were selected in puromycin. Primary mouse brain pericytes were isolated as previously described (32). All cell lines were routinely tested for mycoplasma by PCR and tested negative.

Transwell migration assay

10T1/2 cells (7.5×10^5) or mouse brain pericytes (7.5×10^5) on their own or with sEND endothelial cells (5×10^5) plated on the abluminal side of the filter, were plated in pericyte medium onto the upper chamber of 24mm 8.0 μ m pore Matrigel-coated Transwell filters (Corning) for 24 hours. 24 hours later, 4T1-RFP cells (5×10^5) were added to the upper chamber in 2% FCS supplemented AdvDMEM,

with 20% FCS supplemented AdvDMEM in the bottom chamber. 24 hours later, Transwells were washed, transmigrated cells detached in trypsin/EDTA and 4T1-RFP cell number quantified on LSRII FACS analyzer.

HUVEC (1×10^5) were seeded onto the upper chamber of 6.5 mm/8.0 μm 0.2% gelatin-coated Transwells (Corning) overnight. Human brain pericytes (BP) (2×10^4) were added to the upper chamber. 5 hours later, MDA-MB-231-LM2 cells (1×10^4 , stained with PKH67 red fluorescent dye (Sigma)) were added to the upper chamber in 2% FCS supplemented GlutaMAX with 10% FCS supplemented GlutaMAX in the bottom chamber. 6 hours later, Transwells were washed, fixed with Roti-Histofix 4% for 10 minutes and cell number analyzed by fluorescent microscopy (10x magnification, 6 fields per filter) and quantified by ImageJ. Where indicated, BP were replaced with BP conditioned medium.

Cell adhesion assay

shNT or shEN 10T1/2 cells (1.5×10^5) or isolated mouse brain pericytes (1.5×10^5) were seeded in 24-well plates and were allowed to form a confluent monolayer. 4T1-RFP cells (7.5×10^4) were seeded on top and allowed to adhere for 15 or 30 minutes. Non-adhered 4T1-RFP cells were removed by washing, remaining cells were detached and analyzed by FACS.

Patient samples

The German study was registered at the tissue bank of the National Center for Tumor Diseases (NCT, Heidelberg, Germany) and performed according to the declaration of Helsinki; written informed consent was obtained from all patients. All patient specimen and corresponding clinical information were exclusively provided in a pseudonymized form according to the Standard Operating Procedures of the NCT, approved by the ethic committee of the University of Heidelberg (Ethics Votes #206/207, year 2005). The UK sample collection was approved by the research ethics committee of the Royal Marsden NHS Foundation Trust.

Statistical analysis

Statistics were performed using GraphPad Prism 6. Unless otherwise stated, all numerical data are expressed mean±standard error of the mean (SEM). All comparisons between 2 groups were made using the two-tailed, unpaired Student's *t*-test, if not indicated otherwise. Unless otherwise stated in the figure legend, *= $P<0.05$, **= $P<0.01$ and ***= $P<0.001$.

RESULTS

Stromal expression of endosialin does not affect primary tumor growth but promotes spontaneous metastasis

To investigate the role of stromal endosialin on tumor metastasis, we compared growth and metastatic progression of orthotopic syngeneic 4T1 mammary tumors in BALB/c wildtype (WT) and endosialin-deficient (EN^{KO}) mice. Confocal microscopy and gene expression profiling of 4T1 tumors revealed that endosialin expression on the tumor vasculature was restricted to pericytes with no detectable expression on endothelial cells (Supplementary Fig. S1). No significant differences in primary tumor growth were detected (Fig. 1A), nor in primary tumor weight at necropsy (Supplementary Fig. S2A). In contrast, there was a significant reduction in spontaneous metastasis in EN^{KO} compared to WT mice, as monitored by tumor burden in the lungs (Fig. 1B and C). Metastatic progression was limited in these experiments by the growth of the primary tumor. To circumvent this limitation and better mimic the clinical setting, 4T1 primary tumors were surgically resected at small size (day 9; ~100mm³) and metastatic progression was traced until mice were culled for ethical reasons or the experiment terminated. Consistent with the data in Fig. 1A, there was no significant difference in the weight of the primary tumors at resection (Supplementary Fig. S2B). However, only 30.7% of WT mice, compared to 70.0% of EN^{KO} mice, survived to termination of the experiment (day 93, Fig. 1D). Examination of lung metastatic burden revealed a significantly reduced number of pulmonary tumor nodules in EN^{KO} compared to WT mice (Fig. 1E). Of note, surviving mice at the end of the experiment had no detectable metastatic disease in the lungs.

To exclude possible adaptive immunity related effects in the observed metastasis phenotype, we next performed 4T1 metastasis experiments in Swiss nude WT and EN^{KO} immunocompromised mice. Again, there was no significant difference in primary tumor growth (Fig. 1F and G; Supplementary Fig. S2C). However, metastatic burden as monitored by *ex vivo* IVIS imaging was significantly reduced in EN^{KO} mice (Fig. 1H). Moreover, IVIS imaging of individual organs revealed a significant reduction in metastasis not just to the lungs, but also to liver, lymph nodes, spleen, brain

and bone (Fig. 1H and I; Supplementary Fig. S2D-I), indicating that the decrease in metastasis in BALB/c EN^{KO} mice was not dependent on an intact immune system.

To validate the 4T1 metastasis phenotype in a second tumor model, Lewis lung carcinoma (LLC) cells were grown subcutaneously in C57BL/6 WT and EN^{KO} mice and tumors were surgically resected at day 16 (~300mm³). As with the 4T1 tumors, endosialin expression in the LLC tumor vasculature was restricted to pericytes (Supplementary Fig. S1C). There was no significant difference in primary tumor growth (Fig. 2A), but there was a significant reduction in the number of EN^{KO} mice with histologically detectable metastases in the lungs upon termination of the experiment (day 35; Fig. 2B and C).

Endosialin does not affect metastatic seeding or colonization

Based on the prominent metastasis phenotype in the absence of an overt primary tumor phenotype, we hypothesized that stromal endosialin might affect metastatic seeding and/or colonization. Consequently, we studied metastatic colonization upon tail vein injection of 4T1 (Fig. 3A-D) or LLC (Fig. 3E and F) cells in WT and EN^{KO} mice. There was no difference in lung tumor burden between experimental groups in either tumor model, indicating that stromal endosialin plays no role in metastatic seeding or colonization.

Primary tumors in EN^{KO} mice show no defects in stromal architecture

The exclusion of an effect of endosialin on metastatic seeding and colonization prompted us to analyze in greater detail stromal attributes of primary tumors grown in WT and EN^{KO} mice. In particular, given the well documented upregulation of endosialin expression on pericytes in the tumor vasculature (9-13), we examined the architecture and functionality of tumor vessels. 4T1 primary tumors grown in BALB/c (Fig. 4A and B; Supplementary Fig. S3A and B) and immunocompromised mice (Fig. 4D and E) or LLC primary tumors (Supplementary Fig. S3C and D) revealed no significant differences in the number of tumor microvessels, total vessel area, vessel caliber distribution or deposition of collagen IV in the vascular basement membrane between WT

and EN^{KO} mice. Likewise, vessel maturation, as assessed by pericyte coverage through α SMA and desmin staining, did not differ in tumors grown in WT or EN^{KO} mice (Fig. 4C and F; Supplementary Fig. S3E and F). Similarly, functional experiments showed no difference in vessel perfusion (data not shown) or permeability as monitored by leakage of Hoechst dye (Fig. 4G and H) or Evans blue (Supplementary Fig. S4A and B). Consistent with the indistinguishable structural and functional vessel attributes, primary tumor hypoxia, necrosis, tumor cell proliferation or apoptosis did not differ between WT and EN^{KO} mice in either tumor model (Fig. 4I-L, Supplementary Fig. S4C-G). Finally, given that endosialin is also expressed by myofibroblasts, we assessed stromal collagen deposition in the primary tumors by Sirius red staining and the distribution and abundance of α SMA-positive myofibroblasts, which again showed no differences between the experimental groups (Supplementary Fig. S4H-J). Taken together, these studies revealed no discernible structural stromal differences between tumors in WT and EN^{KO} mice that could account for the prominent metastatic phenotype of endosialin-deficient mice.

Stromal endosialin promotes tumor cell intravasation

A key role of pericytes is in stabilizing the normal vasculature (33). Given the striking upregulation of endosialin expression on tumor-associated pericytes (9-13), we next addressed whether tumor cells displayed an altered propensity to intravasate into the vasculature in WT and EN^{KO} mice. Consistent with the data in Figure 1, 4T1 primary tumor growth was indistinguishable between the experimental groups, but EN^{KO} mice showed a significant reduction of spontaneous lung metastasis as monitored by digital droplet PCR (Fig. 5A and B). Importantly, tumor cell colonies derived from arterial blood were significantly reduced in EN^{KO} mice (Fig. 5C and D), indicating that stromal endosialin regulates intravasation of tumor cells from the primary tumor into the circulation.

To test this hypothesis directly, we performed *in vitro* tumor cell transmigration assays across a pericytes monolayer (Supplementary Fig. S5A and B). 10T1/2 pericyte-like cells expressing non-targeting (shNT) or endosialin-targeting (shEN) shRNAs (Fig. 6A; Supplementary Fig. S6A) were cultured on Matrigel-coated Transwell filters for 24 hours prior to addition of 4T1-RFP tumor cells.

Transmigrated cells were quantified 24 hours later by FACS analysis. The presence of endosialin-expressing shNT 10T1/2 cells, but not shEN 10T1/2 cells with downregulated endosialin expression, enhanced transmigration of 4T1-RFP cells (Fig. 6B). To ensure that these effects were not restricted to 10T1/2 cells, the experiment was repeated using pericytes isolated from the brains of non-tumor bearing WT and EN^{KO} mice (Fig. 6C and D; Supplementary Fig. S6B). Again, the presence of WT pericytes, but not EN^{KO} pericytes, enhanced the transmigration of co-cultured 4T1-RFP cells (Fig. 6D). To validate the tumor cell transmigration enhancing effect of pericyte-expressed endosialin, we examined the ability of human MDA-MB-231 breast cancer cells to transmigrate across a layer of shNT or shEN human brain pericytes (Supplementary Fig. S6C-E). As with the mouse cell experiments, the presence of shNT-human pericytes, but not shEN-pericytes, promoted transmigration of the co-cultured human tumor cells (Fig. 6E).

Finally, to closer model tumor cell intravasation, we mimicked the 3D assembly of the normal vessel wall by allowing tumor cells to transmigrate across sandwich-cultured HUVEC or microvascular endothelial cells and pericytes (Supplementary Fig. S5C and D). As in tumors (see Supplementary Fig. S1) neither HUVEC (9) nor microvascular endothelial cells (Supplementary Fig. S7A) express endosialin. The presence of endosialin-expressing pericytes significantly promoted tumor cell transmigration across the endothelial cell monolayer (Fig. 6F). Equivalent results were obtained using mouse microvascular endothelial cells and shEN or shNT 10T1/2 cells (Supplementary Fig. S7B). Notably, there was no difference between tumor cell transmigration across the endothelial monolayer in the presence of pericytes with downregulated endosialin expression and across an endothelial cell monolayer without pericytes, indicating that endosialin-expressing pericytes actively promote tumor cell intravasation into the vasculature.

Stromal cell endosialin effects on tumor cell intravasation are cell contact-dependent

To shed further insights into the mechanism by which stromal endosialin promotes tumor cell intravasation, we performed transmigration experiments in the presence of pericyte-conditioned medium (Supplementary Fig. S5E). The promotion of tumor cell transmigration by endosialin-

expressing pericytes could not be recapitulated by replacing pericytes with pericyte-conditioned medium (Fig. 6G) indicating that enhanced tumor cell migration was not solely dependent on promigratory factors secreted by endosialin-positive pericytes. Consequently, we set out to determine, if endosialin mediated direct cell-cell interactions between pericytes and tumor cells. To this end, we performed adhesion assays with both shNT and shEN 10T1/2 pericyte-like cells and brain pericytes isolated from WT and EN^{KO} mice. With both cells types, adhesion of 4T1-RFP cells was significantly impaired by downregulation or genetic deletion of endosialin (Fig. 6H and I).

Finally, we investigated whether a pericyte remodeled matrix could substitute for the promigratory cell-cell contact dependent phenotype observed with intact pericytes. 10T1/2 cells and isolated brain pericytes were allowed to remodel the matrix of Matrigel-coated Transwell filters, prior to decellularization by ammonium hydroxide treatment (Supplementary Fig. S5F). Notably, the enhanced transmigratory phenotype of 4T1-RFP cells co-cultured with live shNT pericytes was not recapitulated by a pericyte-remodeled matrix (Supplementary Fig. S7C). Similarly, the increased adhesion of 4T1 cells to WT pericytes was not recapitulated in an adhesion assay where WT pericytes were replaced by WT pericyte-derived extracellular matrix (Supplementary Fig. S7D). These data indicate that the presence of live endosialin-expressing pericytes is required to induce the promigratory, cell-cell contact dependent intravasation phenotype of tumor cells.

Endosialin expression on primary human carcinoma samples primes for metastatic spread

Based on the prominent role of stromal endosialin in mediating metastasis in preclinical mouse models, we assessed the clinical relevance of these experimental findings. First, comparison of microdissected breast tumor stroma and normal adjacent stroma displayed a significantly higher level of endosialin (*CD248*) mRNA in the tumor stroma (Fig. 7A). Next, we stained human primary invasive breast cancer samples with two independent anti-endosialin monoclonal antibodies (B1/35 and FB5) (9). As illustrated in Figure 7B, variable expression of endosialin was detected on tumor pericytes and stromal myofibroblasts. However, with the exception of a rare subset of metaplastic breast cancers, no endosialin expression was detected on tumor cells. When comparing endosialin

protein and *CD248* mRNA levels in the primary tumor with the metastatic stage, a significant correlation was observed between endosialin protein (Fig. 7C; Supplementary Fig. S8A) and mRNA levels (Fig. 7D) with increased incidence of metastasis. In particular, higher *CD248* expression in the primary tumor was found in patients with distant metastasis to the lung, liver and bone as compared to patients without detectable metastatic disease (Supplementary Fig. S8B). Importantly, examination of *CD248* expression in microdissected breast tumor stroma (34) revealed a significant association between high stromal *CD248* expression and decreased recurrence-free survival (Fig. 7E), whereas high *CD248* expression in a dataset of 334 lymph-node positive breast cancers (35) was significantly associated with decreased distant metastasis-free survival (Fig. 7F). Taken together, these data indicate that endosialin expression in the primary tumor serves as poor prognostic factor for the development of metastatic disease.

DISCUSSION

Endosialin (CD248) is a mesenchymal cell surface receptor that is widely expressed during embryonic development and downregulated in healthy adult tissues (10,11,14,25). Endosialin may be abundantly expressed in the adult upon pathological challenge, most notably by pericytes and myofibroblasts in the tumor-associated stroma (7,9,11,12,14) as well as in fibrotic (26) and atherosclerotic tissues (HGA, unpublished data). Although endosialin was originally named TEM1 (tumor endothelial marker 1) (6,8), this was later shown to be a misleading nomenclature when different laboratories reported endosialin expression being restricted to stromal pericytes and myofibroblasts and absent from endothelial cells of various human and mouse tumors (9,11,12,25,36). The downregulated expression in the adult in combination with the striking upregulation in tumors makes endosialin an oncofetal protein that is in principle, strictly based on its unique pathology-associated expression pattern, an attractive therapeutic target. Indeed, we demonstrate here, in three different pre-clinical models that stromal endosialin expression facilitates spontaneous distant site metastasis. To mechanistically unravel the role of stromal endosialin during individual steps of tumor progression and metastasis, we set out comparative tumor experiments in wildtype (WT) and endosialin-deficient (EN^{KO}) mouse models and in 3D *in vitro* reconstitution assays. Complementing these studies with the analysis of human breast cancer expression datasets, we show that (i) enhanced spontaneous metastasis in WT mice requires upregulated endosialin expression on tumor-associated pericytes to promote tumor cell intravasation into the circulation, (ii) endosialin mediates direct cell-cell interactions of tumor-associated pericytes and tumor cells to promote tumor cells transmigration across an endothelial monolayer, and (iii) breast cancer patients with high primary tumor endosialin expression have significantly higher rates of metastasis and reduced recurrence-free survival.

Previous studies addressing the role of pericytes in tumorigenesis have focused on ablating pericytes (37,38) or blockade of PDGFR β signaling in pericytes by genetic targeting (31), pharmacological inhibition (39), PDGFR β blocking antibodies (37,40) or PDGF-B binding oligonucleotide aptamers (41). All these strategies resulted in loss of pericyte coverage on the tumor

vasculature, subsequent vascular destabilization and, in most cases, a reduction in tumor volume. Intriguingly, where it was examined, this vascular destabilization and inhibition of tumor growth, potentially enhancing tumor hypoxia and inducing tumor cell EMT, was accompanied by increased metastatic spread (31,37,38). Indeed, low pericyte coverage in clinical samples is associated with poor patient prognosis (42,43). These findings are reminiscent of recent studies demonstrating that two independent genetic strategies to reduce myofibroblasts in the stroma of pancreatic cancers resulted in enhanced tumor aggressiveness (44,45). However, while genetic deletion of *Shh* resulted in enhanced tumor growth (45), pharmacological targeting of the Hh pathway improved drug delivery and reduced tumor invasion and metastasis (46,47). These contrasting data reinforce the notion that stromal effects on tumor progression and metastasis may be highly contextual and that stromal cells can play both tumor promoting and tumor suppressing roles dependent on the tumor type and location. This has led to the concept that it may be more effective to deploy strategies to "normalize" or de-differentiate tumor-associated stromal cells rather than target them for destruction.

Consistent with this concept, unlike targeting PDGFR β or ablating pericytes, treatment of syngeneic tumor bearing human *CD248* knock-in mice with the anti-human endosialin antibody MORAb-004 did not result in a reduction in vessel number or destabilization of the vasculature, as monitored by endothelial cell viability, pericyte coverage and integrity of the basement membrane, but significantly impaired the growth of B16-F10 tumors following subcutaneous or intravenous inoculation (36). Importantly, in the study reported here, the impairment in metastatic dissemination in the EN^{KO} mice was not associated with gross alterations in the tumor vasculature. Primary tumors in both syngeneic and immunocompromised WT and EN^{KO} mice were indistinguishable in terms of vessel architecture including, as previously observed in the developing retinal vasculature of EN^{KO} mice (28), no detectable loss in pericyte coverage. Similarly, there were no significant differences in vascular patency in WT and EN^{KO} tumors as monitored by vessel perfusion, vascular leakage and levels of primary tumor hypoxia and necrosis, indicating that an inability to upregulate endosialin expression in the tumor stroma has minimal impact on vascular integrity. Importantly, in primary

tumors from EN^{KO} mice, the number or distribution of α SMA-expressing myofibroblasts was not altered suggesting that the expression of endosialin by myofibroblasts is not the driving force of tumor cell dissemination and intravasation. Consistent with this lack of stromal disruption, no differences in primary tumor growth in WT and EN^{KO} mice were detected in the three tumor models used in this study. Previous studies also reported no differences in LLC or B16-F0 subcutaneous primary tumor growth in WT and EN^{KO} mice (27,28) or following intracranial inoculation of C57MG glioblastoma cells (30). In contrast, when HCT116 colorectal tumor fragments were orthotopically grafted onto the intestinal surface, tumors in the EN^{KO} mice were reduced in volume and showed reduced local invasion and metastasis (27). The mechanism underlying these effects was not investigated, but the data demonstrate that stromal endosialin modulation of primary tumor growth may vary depending on the tumor site and the conditions of the microenvironment.

To relate endosialin to distinct steps of the metastatic cascade, we performed seeding and colonization experiments by intravenous injection of tumor cells. These experiments revealed unambiguously that endosialin was not involved in secondary site colonization. We therefore focused on the intravasation of cells from the primary tumor as a possible rate-limiting step of metastasis. Indeed, while microvessel permeability were indistinguishable in primary tumors grown in WT and EN^{KO} mice, the expression of endosialin had a pronounced effect on the ability of tumor cells to enter the systemic blood circulation. Of note, we observed in comparative studies a reduction in spontaneous metastasis in both EN^{KO} immunocompetent and immunocompromised mice, which ruled out an involvement of an intact immune system as an effector of the endosialin-mediated metastasis phenotype. Recently, the presence of macrophages at tumor cell intravasation sites has been shown to promote tumor cell intravasation (48,49), however, analysis of tumors growing in WT or EN^{KO} mice did not yield any significant differences in macrophage numbers indicating that macrophages are not the driving force for endosialin-mediated tumor cell intravasation (C.K. & H.G.A., unpublished data). In conclusion, although the mechanisms of tumor cell intravasation are not well elucidated, these data indicate that the interaction of tumor cells with both pericytes and endothelial cells may play a role (50).

To delineate more directly the roles of individual cell populations, we mimicked the multicellular vascular crosstalk in a modified Transwell migration assay. Pericytes with or without endosialin expression were co-cultured with endothelial cells, and tumor cells were analyzed for their ability to transmigrate across the endothelial layer. These *in vitro* reconstruction experiments validated the *in vivo* findings to show that endosialin expression by pericytes alone stimulated tumor cell transmigration. Importantly, this stimulatory behavior of endosialin-positive pericytes was independent of the effect of pericytes on endothelial cells as enhanced tumor cell transmigration was still observed in the absence of an endothelial monolayer. Moreover, this ability of endosialin-positive pericytes to promote tumor cell transmigration could not be recapitulated by pericyte conditioned medium or pericyte remodeled extracellular matrix indicating a requirement for a direct interaction between tumor cells and tumor pericytes during intravasation. While the detailed molecular mechanisms mediating this interaction await elucidation, analysis of global gene expression data of primary tumor cells isolated from WT and EN^{KO} tumor-bearing mice indicate that endosialin-positive stroma does not alter the intrinsic tumor cell transcriptional profile (C.V. & C.M.I., unpublished data), rather that it functions to modulate the local microenvironment. Indeed, it has been reported previously that recombinant endosialin can bind in *in vitro* assays to extracellular matrix components, including collagen and fibronectin (24), and *in vivo* to the vascular basement membrane (28). Thus, based on the available data, we hypothesize that endosialin does not function as an active metastasis promoting signaling factor in educating tumor cells to gain invasive behavior, but rather as a facilitator tethering tumor cells to the matrix and actively mediating their transmigration through the vascular basement membrane and underlying endothelial monolayer.

In conclusion, the data presented here causally link the expression of a metastasis-facilitating stromal receptor to a very specific step of the metastatic cascade and shed important mechanistic insight into the role of tumor-associated pericytes in mediating tumor metastasis. Importantly, the clinical relevance of these preclinical tumor experiments, involving independent tumor models with corresponding mechanistic cellular experiments could be validated by comparative pathology of human tumors. Indeed, analysis of human breast cancer samples revealed that the abundance of

primary tumor stromal endosialin expression strongly correlated with metastatic progression and reduced recurrence-free survival. Consequently, the findings of this study and the unique oncofetal expression of endosialin warrant further consideration of endosialin as a therapeutic target to limit tumor progression and metastasis.

ACKNOWLEDGEMENTS

We would like to thank Dr. David Huso (Johns Hopkins University, Baltimore, USA) for providing EN^{KO} mice. We gratefully acknowledge David Robertson, Marjan Iravani, Qiong Gao, Nicole Simonavicius and the Histopathology Facility (Breast Cancer Now Research Center), and Maria Riedel (DKFZ) and Eva Besemfelder (DKFZ) for their assistance and support in this project. We would also like to thank the excellent technical support by the DKFZ Laboratory and Institute of Cancer Research Animal and Imaging core facilities.

REFERENCES

1. Massague J, Obenauf AC. Metastatic colonization by circulating tumour cells. *Nature* 2016;529(7586):298-306.
2. Fidler IJ. The pathogenesis of cancer metastasis: the 'seed and soil' hypothesis revisited. *Nat Rev Cancer* 2003;3(6):453-8.
3. Joyce JA, Pollard JW. Microenvironmental regulation of metastasis. *Nat Rev Cancer* 2009;9(4):239-52.
4. Gerhardt H, Semb H. Pericytes: gatekeepers in tumour cell metastasis? *J Mol Med (Berl)* 2008;86(2):135-44.
5. Pietras K, Ostman A. Hallmarks of cancer: interactions with the tumor stroma. *Exp Cell Res* 2010;316(8):1324-31.
6. Christian S, Ahorn H, Koehler A, Eisenhaber F, Rodi HP, Garin-Chesa P, et al. Molecular cloning and characterization of endosialin, a C-type lectin-like cell surface receptor of tumor endothelium. *J Biol Chem* 2001;276(10):7408-14.
7. Rettig WJ, Garin-Chesa P, Healey JH, Su SL, Jaffe EA, Old LJ. Identification of endosialin, a cell surface glycoprotein of vascular endothelial cells in human cancer. *Proc Natl Acad Sci U S A* 1992;89(22):10832-6.
8. St Croix B, Rago C, Velculescu V, Traverso G, Romans KE, Montgomery E, et al. Genes expressed in human tumor endothelium. *Science* 2000;289(5482):1197-202.
9. MacFadyen JR, Haworth O, Roberston D, Hardie D, Webster MT, Morris HR, et al. Endosialin (TEM1, CD248) is a marker of stromal fibroblasts and is not selectively expressed on tumour endothelium. *FEBS Lett* 2005;579(12):2569-75.
10. MacFadyen J, Savage K, Wienke D, Isacke CM. Endosialin is expressed on stromal fibroblasts and CNS pericytes in mouse embryos and is downregulated during development. *Gene Expr Patterns* 2007;7(3):363-9.
11. Christian S, Winkler R, Helfrich I, Boos AM, Besemfelder E, Schadendorf D, et al. Endosialin (Tem1) is a marker of tumor-associated myofibroblasts and tumor vessel-associated mural cells. *Am J Pathol* 2008;172(2):486-94.
12. Simonavicius N, Robertson D, Bax DA, Jones C, Huijbers IJ, Isacke CM. Endosialin (CD248) is a marker of tumor-associated pericytes in high-grade glioma. *Mod Pathol* 2008;21(3):308-15.

13. Rouleau C, Curiel M, Weber W, Smale R, Kurtzberg L, Mascarello J, et al. Endosialin protein expression and therapeutic target potential in human solid tumors: sarcoma versus carcinoma. *Clin Cancer Res* 2008;14(22):7223-36.
14. Rupp C, Dolznig H, Puri C, Sommergruber W, Kerjaschki D, Rettig WJ, et al. Mouse endosialin, a C-type lectin-like cell surface receptor: expression during embryonic development and induction in experimental cancer neoangiogenesis. *Cancer Immun* 2006;6:10.
15. Huber MA, Kraut N, Schweifer N, Dolznig H, Peter RU, Schubert RD, et al. Expression of stromal cell markers in distinct compartments of human skin cancers. *J Cutan Pathol* 2006;33(2):145-55.
16. Brady J, Neal J, Sadakar N, Gasque P. Human endosialin (tumor endothelial marker 1) is abundantly expressed in highly malignant and invasive brain tumors. *J Neuropathol Exp Neurol* 2004;63(12):1274-83.
17. O'Shannessy DJ, Somers EB, Chandrasekaran LK, Nicolaides NC, Bordeaux J, Gustavson MD. Influence of tumor microenvironment on prognosis in colorectal cancer: Tissue architecture-dependent signature of endosialin (TEM-1) and associated proteins. *Oncotarget* 2014;5(12):3983-95.
18. Chacko AM, Li C, Nayak M, Mikitsh JL, Hu J, Hou C, et al. Development of 124I immuno-PET targeting tumor vascular TEM1/endosialin. *J Nucl Med* 2014;55(3):500-7.
19. Rouleau C, Gianolio DA, Smale R, Roth SD, Krumbholz R, Harper J, et al. Anti-Endosialin Antibody-Drug Conjugate: Potential in Sarcoma and Other Malignancies. *Mol Cancer Ther* 2015;14(9):2081-9.
20. Kiyohara E, Donovan N, Takeshima L, Huang S, Wilmott JS, Scolyer RA, et al. Endosialin Expression in Metastatic Melanoma Tumor Microenvironment Vasculature: Potential Therapeutic Implications. *Cancer Microenviron* 2015;8(2):111-8.
21. Diaz LA, Jr., Coughlin CM, Weil SC, Fishel J, Gounder MM, Lawrence S, et al. A first-in-human phase I study of MORAb-004, a monoclonal antibody to endosialin in patients with advanced solid tumors. *Clin Cancer Res* 2015;21(6):1281-8.
22. Tomkowicz B, Rybinski K, Sebeck D, Sass P, Nicolaides NC, Grasso L, et al. Endosialin/TEM-1/CD248 regulates pericyte proliferation through PDGF receptor signaling. *Cancer Biol Ther* 2010;9(11):908-15.
23. Lax S, Hardie DL, Wilson A, Douglas MR, Anderson G, Huso D, et al. The pericyte and stromal cell marker CD248 (endosialin) is required for efficient lymph node expansion. *Eur J Immunol* 2010;40(7):1884-9.
24. Tomkowicz B, Rybinski K, Foley B, Ebel W, Kline B, Routhier E, et al. Interaction of endosialin/TEM1 with extracellular matrix proteins mediates cell adhesion and migration. *Proc Natl Acad Sci U S A* 2007;104(46):17965-70.

25. Bagley RG, Honma N, Weber W, Boutin P, Rouleau C, Shankara S, et al. Endosialin/TEM 1/CD248 is a pericyte marker of embryonic and tumor neovascularization. *Microvasc Res* 2008;76(3):180-8.
26. Mogler C, Wieland M, König C, Hu J, Runge A, Korn C, et al. Hepatic stellate cell-expressed endosialin balances fibrogenesis and hepatocyte proliferation during liver damage. *EMBO Mol Med* 2015;7(3):332-8.
27. Nanda A, Karim B, Peng Z, Liu G, Qiu W, Gan C, et al. Tumor endothelial marker 1 (Tem1) functions in the growth and progression of abdominal tumors. *Proc Natl Acad Sci U S A* 2006;103(9):3351-6.
28. Simonavicius N, Ashenden M, van Weverwijk A, Lax S, Huso DL, Buckley CD, et al. Pericytes promote selective vessel regression to regulate vascular patterning. *Blood* 2012;120(7):1516-27.
29. Naylor AJ, McGettrick HM, Maynard WD, May P, Barone F, Croft AP, et al. A differential role for CD248 (Endosialin) in PDGF-mediated skeletal muscle angiogenesis. *PLoS One* 2014;9(9):e107146.
30. Carson-Walter EB, Winans BN, Whiteman MC, Liu Y, Jarvela S, Haapasalo H, et al. Characterization of TEM1/endosialin in human and murine brain tumors. *BMC Cancer* 2009;9:417.
31. Xian X, Hakansson J, Stahlberg A, Lindblom P, Betsholtz C, Gerhardt H, et al. Pericytes limit tumor cell metastasis. *J Clin Invest* 2006;116(3):642-51.
32. Tigges U, Welser-Alves JV, Boroujerdi A, Milner R. A novel and simple method for culturing pericytes from mouse brain. *Microvasc Res* 2012;84(1):74-80.
33. Armulik A, Abramsson A, Betsholtz C. Endothelial/pericyte interactions. *Circ Res* 2005;97(6):512-23.
34. Finak G, Bertos N, Pepin F, Sadekova S, Souleimanova M, Zhao H, et al. Stromal gene expression predicts clinical outcome in breast cancer. *Nat Med* 2008;14(5):518-27.
35. Gyorffy B, Lanczky A, Szallasi Z. Implementing an online tool for genome-wide validation of survival-associated biomarkers in ovarian-cancer using microarray data from 1287 patients. *Endocr Relat Cancer* 2012;19(2):197-208.
36. Rybinski K, Imtiyaz HZ, Mittica B, Drozdowski B, Fulmer J, Furuuchi K, et al. Targeting endosialin/CD248 through antibody-mediated internalization results in impaired pericyte maturation and dysfunctional tumor microvasculature. *Oncotarget* 2015;6(28):25429-40.
37. Cooke VG, LeBleu VS, Keskin D, Khan Z, O'Connell JT, Teng Y, et al. Pericyte depletion results in hypoxia-associated epithelial-to-mesenchymal transition and metastasis mediated by met signaling pathway. *Cancer Cell* 2012;21(1):66-81.
38. Keskin D, Kim J, Cooke VG, Wu CC, Sugimoto H, Gu C, et al. Targeting vascular pericytes in hypoxic tumors increases lung metastasis via angiopoietin-2. *Cell Rep* 2015;10(7):1066-81.

39. Bergers G, Song S, Meyer-Morse N, Bergsland E, Hanahan D. Benefits of targeting both pericytes and endothelial cells in the tumor vasculature with kinase inhibitors. *J Clin Invest* 2003;111(9):1287-95.
40. Song S, Ewald AJ, Stallcup W, Werb Z, Bergers G. PDGFRbeta+ perivascular progenitor cells in tumours regulate pericyte differentiation and vascular survival. *Nat Cell Biol* 2005;7(9):870-9.
41. Sennino B, Falcon BL, McCauley D, Le T, McCauley T, Kurz JC, et al. Sequential loss of tumor vessel pericytes and endothelial cells after inhibition of platelet-derived growth factor B by selective aptamer AX102. *Cancer Res* 2007;67(15):7358-67.
42. O'Keeffe MB, Devlin AH, Burns AJ, Gardiner TA, Logan ID, Hirst DG, et al. Investigation of pericytes, hypoxia, and vascularity in bladder tumors: association with clinical outcomes. *Oncol Res* 2008;17(3):93-101.
43. Yonenaga Y, Mori A, Onodera H, Yasuda S, Oe H, Fujimoto A, et al. Absence of smooth muscle actin-positive pericyte coverage of tumor vessels correlates with hematogenous metastasis and prognosis of colorectal cancer patients. *Oncology* 2005;69(2):159-66.
44. Ozdemir BC, Pentcheva-Hoang T, Carstens JL, Zheng X, Wu CC, Simpson TR, et al. Depletion of carcinoma-associated fibroblasts and fibrosis induces immunosuppression and accelerates pancreas cancer with reduced survival. *Cancer Cell* 2014;25(6):719-34.
45. Rhim AD, Oberstein PE, Thomas DH, Mirek ET, Palermo CF, Sastra SA, et al. Stromal elements act to restrain, rather than support, pancreatic ductal adenocarcinoma. *Cancer Cell* 2014;25(6):735-47.
46. Olive KP, Jacobetz MA, Davidson CJ, Gopinathan A, McIntyre D, Honess D, et al. Inhibition of Hedgehog signaling enhances delivery of chemotherapy in a mouse model of pancreatic cancer. *Science* 2009;324(5933):1457-61.
47. Khan S, Ebeling MC, Chauhan N, Thompson PA, Gara RK, Ganju A, et al. Ormeloxifene suppresses desmoplasia and enhances sensitivity of gemcitabine in pancreatic cancer. *Cancer Res* 2015;75(11):2292-304.
48. Harney AS, Arwert EN, Entenberg D, Wang Y, Guo P, Qian BZ, et al. Real-Time Imaging Reveals Local, Transient Vascular Permeability, and Tumor Cell Intravasation Stimulated by TIE2hi Macrophage-Derived VEGFA. *Cancer Discov* 2015;5(9):932-43.
49. Pignatelli J, Goswami S, Jones JG, Rohan TE, Pieri E, Chen X, et al. Invasive breast carcinoma cells from patients exhibit MenaINV- and macrophage-dependent transendothelial migration. *Sci Signal* 2014;7(353):ra112.
50. Ribeiro AL, Okamoto OK. Combined effects of pericytes in the tumor microenvironment. *Stem Cells Int* 2015;2015:868475.

FIGURE LEGENDS

Figure 1. Stromal endosialin promotes spontaneous metastasis, while not affecting primary 4T1 tumor growth.

A-E, 4T1 cells (2×10^5) were injected orthotopically into BALB/c WT and EN^{KO} mice. A, Primary tumor growth (n=10-11 per group). B, Quantification of spontaneous lung metastases from 3 sections per mouse. Each data point represents one mouse. *, $P < 0.05$. C, Representative H&E staining of lung sections. Arrowheads indicate metastatic lung lesions. Scale bar, 1mm. D, Kaplan-Meier survival curves after surgical removal of the primary tumor at day 9 or 10 (n=10-13 mice per group). E, Quantification of lung metastasis. *, $P < 0.05$. F-I, 4T1-Luc cells (1×10^6) were orthotopically injected into Swiss nude WT (n=7) or EN^{KO} (n=4) mice. F, Primary tumor growth (see Supplementary Fig. S2C for primary tumor growth of second experiment; WT, n=5; EN^{KO}, n=4). G, Representative *in vivo* IVIS images at day 7. H, Quantification of spontaneous metastasis to organs monitored via *ex vivo* IVIS imaging 14 days after surgical primary tumor removal. Each data point represents one organ (combination of two independent experiments (WT, n=12; EN^{KO}, n=8 mice)); see Supplementary Fig. S2D-I for individual organs; ***, $P = 0.0005$; Mann-Whitney test. I, Representative *ex vivo* IVIS images.

Figure 2. Stromal endosialin promotes spontaneous metastasis of LLC tumors, while not affecting primary tumor growth.

A, LLC cells (1×10^5) were subcutaneously injected into C57BL/6 WT and EN^{KO} mice (n=10-11 mice per group) and allowed to grow for 16 days. B, Percentage of mice with metastases 19 days after surgical primary tumor removal (combination of two independent experiments (n=21 mice per group; *, $P < 0.05$, Fischer's exact test)). C, Representative images of resected lungs with corresponding H&E staining. Arrowheads indicate metastatic lung lesions. Scale bar, 1mm.

Figure 3. Metastatic seeding or colonization is not affected by stromal endosialin.

A-D, 4T1 cells (5×10^4) were injected intravenously into BALB/c WT and EN^{KO} mice (n=9 per group). A, Quantification of tumor burden in lungs from IVIS images (day 14). Each data point represents one

mouse. B, Representative IVIS images. C, Quantification of lung metastatic area. Each data point represents one mouse. D, Representative H&E stained lung sections. Arrowheads indicate metastatic lesions. Scale bar, 1mm. E and F, LLC cells (1×10^6) were injected intravenously into C57BL/6 WT (n=11) and EN^{KO} (n=6) mice. E, Quantification of lung colonization at day 14. Scoring: 0 = no tumor, 1 = small metastatic foci, 2 = large metastatic foci covering 5 to 25% of section, 3 = large metastatic foci covering >25% of section. Each data point represents one mouse. F, Representative images of resected lungs and corresponding H&E sections. Scale bar, 0.5mm.

Figure 4. Vessel architecture and function in the primary tumor is not affected by stromal endosialin. A-C, 4T1 cells (2×10^5) were injected into BALB/c WT and EN^{KO} mice (n=7 per group). A, Endomucin (red) and α SMA (green) stained tumor sections. Scale bar, 100 μ m. B, Quantification blood vessel density from 3 random fields per section. Each data point represents one mouse. C, Pericyte coverage quantified as % of blood vessels associated with α SMA+ pericytes from 3 random fields per section. Each data point represents one mouse. D-F, 4T1-Luc primary tumors in Swiss nude WT and EN^{KO} mice (n=5-6 per group from Fig. 1F). D, CD31 (green) and desmin (red) stained tumor sections. Scale bar, 100 μ m. E, Quantification of CD31+ vessel area per total tumor area. F, Quantification of desmin+ area per total tumor area. G, Quantification of Hoechst dye in 4T1-tumor-bearing WT and EN^{KO} BALB/c mice normalized to blood vessel density (n=4 per group). 3 random fields per tumor section were analyzed. H, Representative images. Scale bar, 100 μ m. I, 4T1 tumor bearing WT (n=11) or EN^{KO} (n=8) BALB/c mice were injected with pimonidazole. Hypoxia was quantified as % of pimonidazole-positive tumor area per total tumor area. Each data point represents one mouse. J-L, 4T1-Luc primary tumors in Swiss nude WT and EN^{KO} mice (n=4-7 per group from Fig. 1F) were sectioned. J, Quantification of necrotic tumor area per total tumor area. K, Quantification of proliferation by Ki67+ cells per high power field of view. Data represents mean values from 5 random fields per tumor section. L, Representative images of Ki67 staining. Scale bar, 50 μ m.

Figure 5. Stromal endosialin promotes tumor cell dissemination.

4T1-Luc-RFP cells (1×10^4) were injected orthotopically into BALB/c WT or EN^{KO} mice (n=11 mice per group). A, Primary tumor growth. B, Quantification of lung metastasis by ddPCR. Data shown are the % RFP+ droplets relative to TFRC+. Each data point represents one mouse. *, $P < 0.05$. C, Quantification of circulating tumor cells from 14 days cultured blood. Data are mean number of tumor colonies per 100 μ L whole blood from 2 independent samples per animal *, $P < 0.05$. Equivalent results were obtained in 2 independent experiments. D, Representative images of tumor cell colonies.

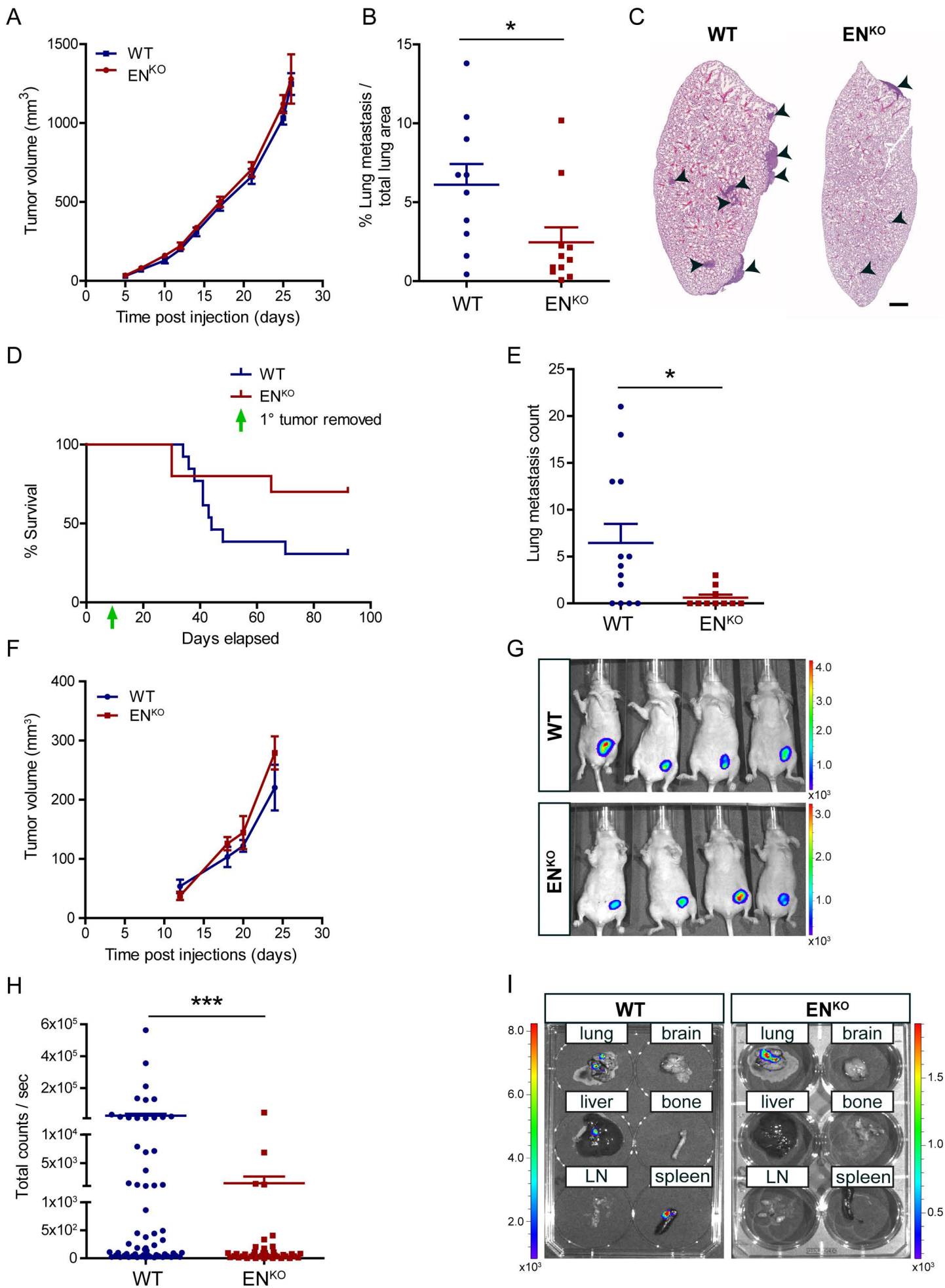
Figure 6. Endosialin-expressing pericytes promote tumor cell intravasation in a cell contact-dependent manner.

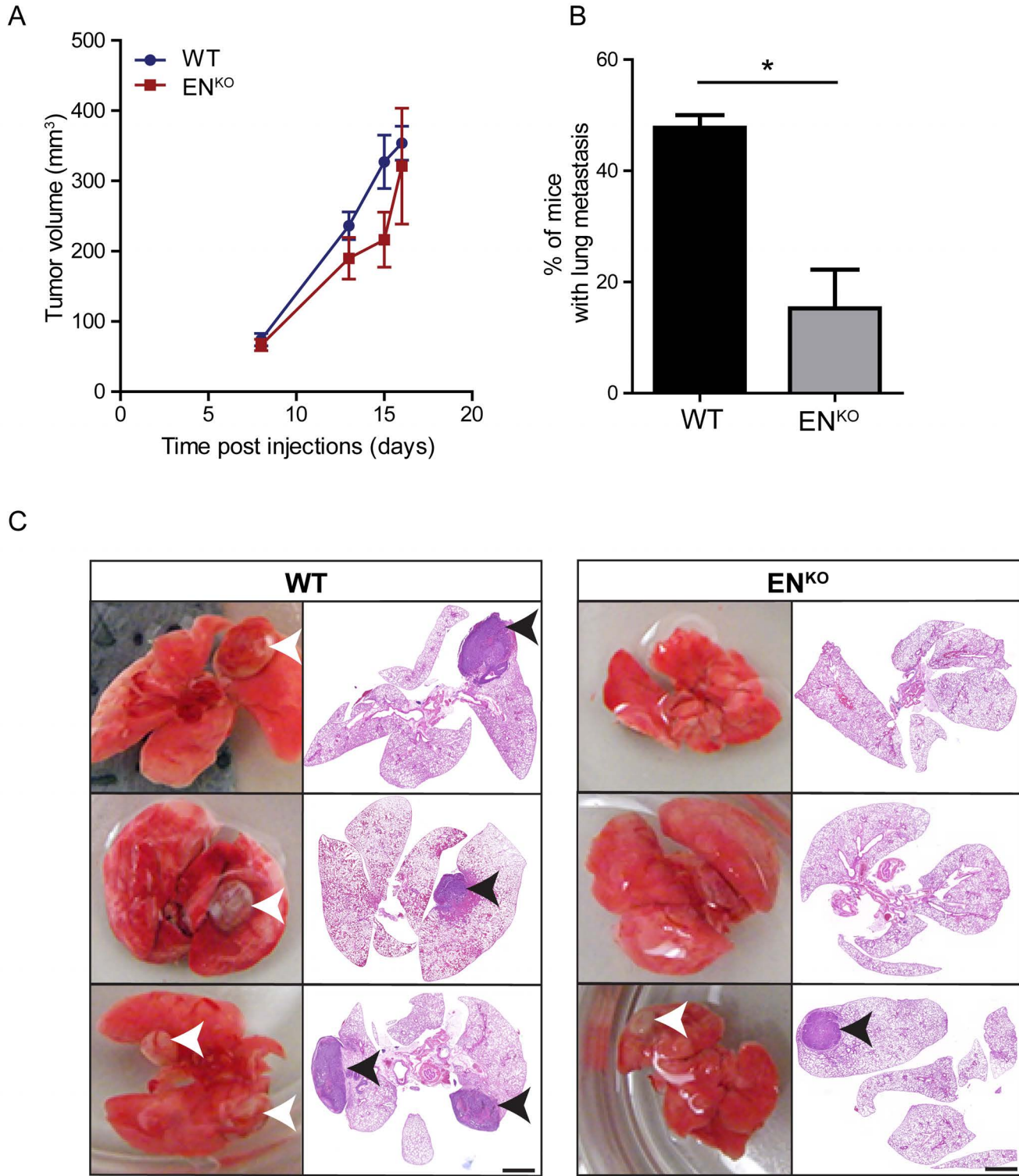
See Supplementary Fig. S5 for experimental setup. A, shNT and shEN 10T1/2 cells stained for endosialin (green) or phalloidin (red). Scale bar, 75 μ m. B, Quantification of transmigrated 4T1-RFP cells through a Transwell layer of shNT and shEN 10T1/2 cells after 24 hours. Control wells contained no 10T1/2 cells. *, $P < 0.05$, one-way ANOVA. C, Brain pericytes isolated from WT or EN^{KO} BALB/c mice stained for endosialin (red) or endomucin (green). Scale bar, 75 μ m. D, Quantification of transmigrated 4T1-RFP cells through a Transwell layer of isolated WT and EN^{KO} pericytes after 24 hours. Data shown are combined from two independent experiments. *, $P < 0.05$, one-way ANOVA. E, Quantification of transmigrated PKH67-labeled MDA-MB-231-LM2 cells through a Transwell layer of shNT or shEN human brain pericytes (BP) after 6 hours. Data shown are combined from 4 independent experiments. *, $P < 0.05$. F, Quantification of MDA-MB-231-LM2 transmigration as described in panel E except that HUVEC were first seeded on gelatin-coated Transwells overnight prior to the addition of BP. Control wells contained no pericytes. Data shown are combined from 5 independent experiments. ***, $P < 0.001$, **, $P < 0.01$. G, Quantification of MDA-MB-231-LM2 transmigration as described in panel F except that instead of BP, conditioned medium from shNT or shEN BP was added to the upper well 5 hours prior to addition of MDA-MB-231-LM2 cells. Data shown are combined from 3 independent experiments. H and I, Adhesion of 4T1-RFP tumor cells to a monolayer of (H) shNT or shEN 10T1/2 cells or (I) WT or EN^{KO} mouse brain pericytes. Data show mean

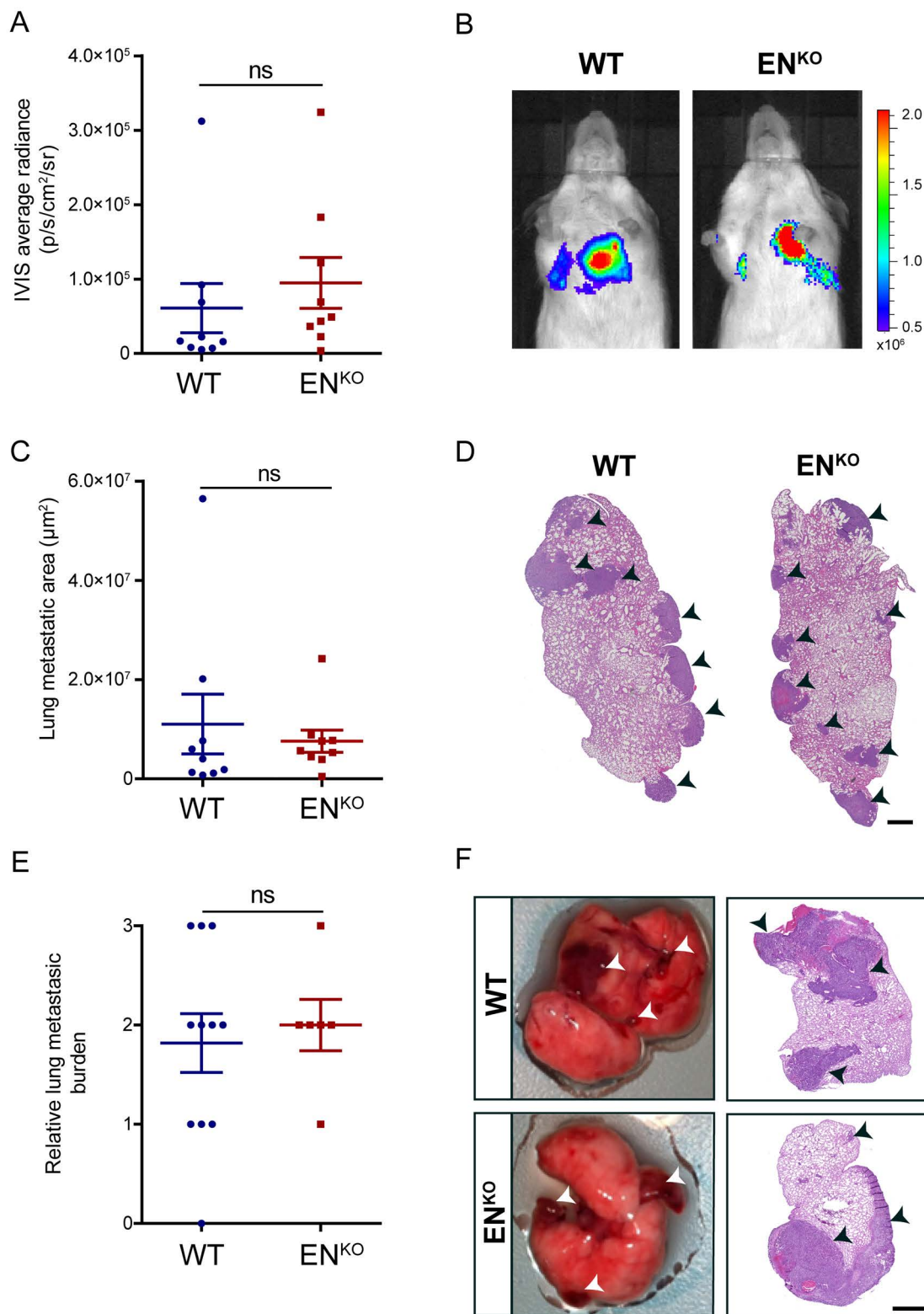
of adherent cells from three wells per condition at each time point. ***, $P<0.001$. Equivalent results were obtained in an independent experiment.

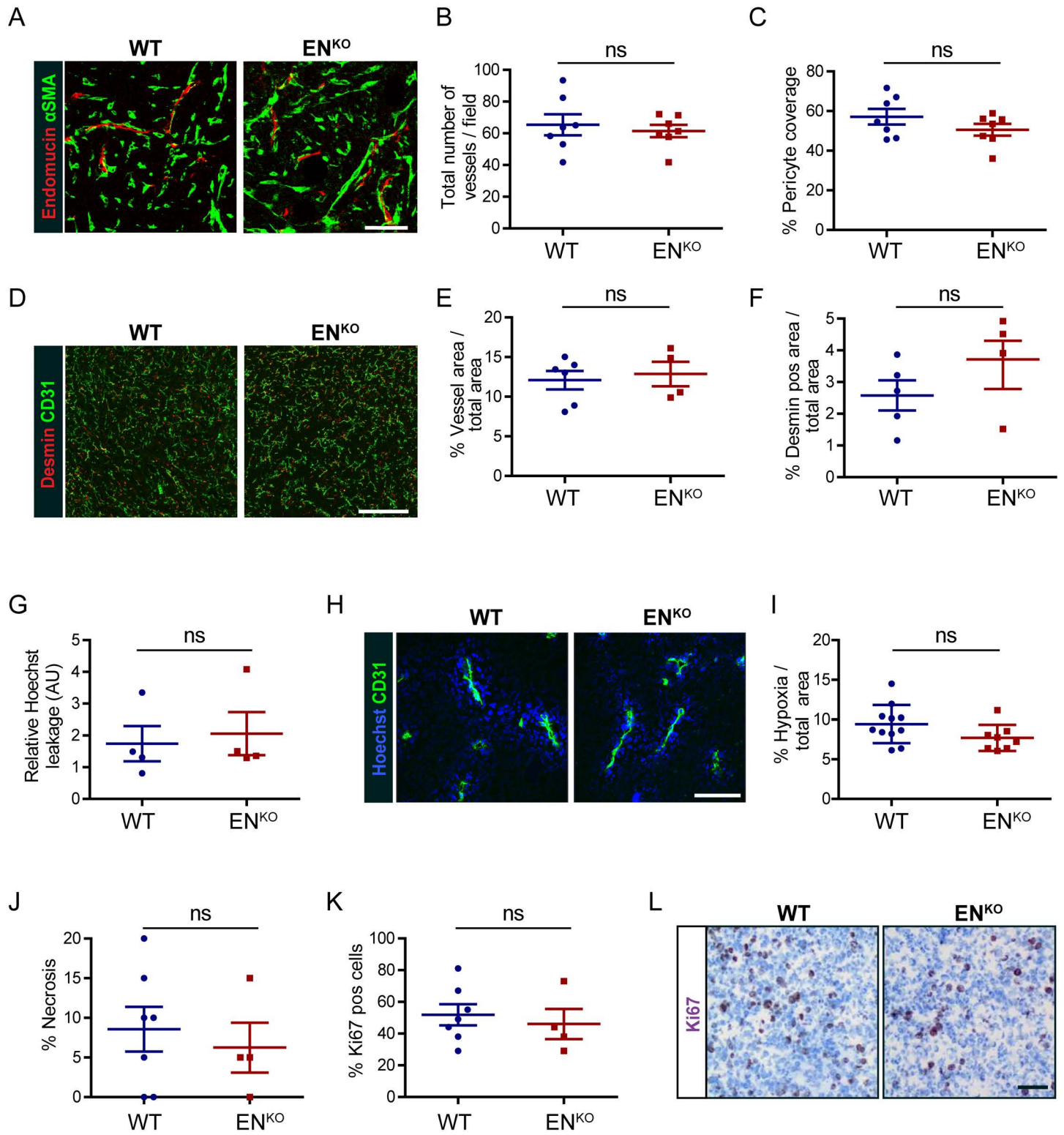
Figure 7. Endosialin expression in primary human breast cancer stroma primes for metastatic spread.

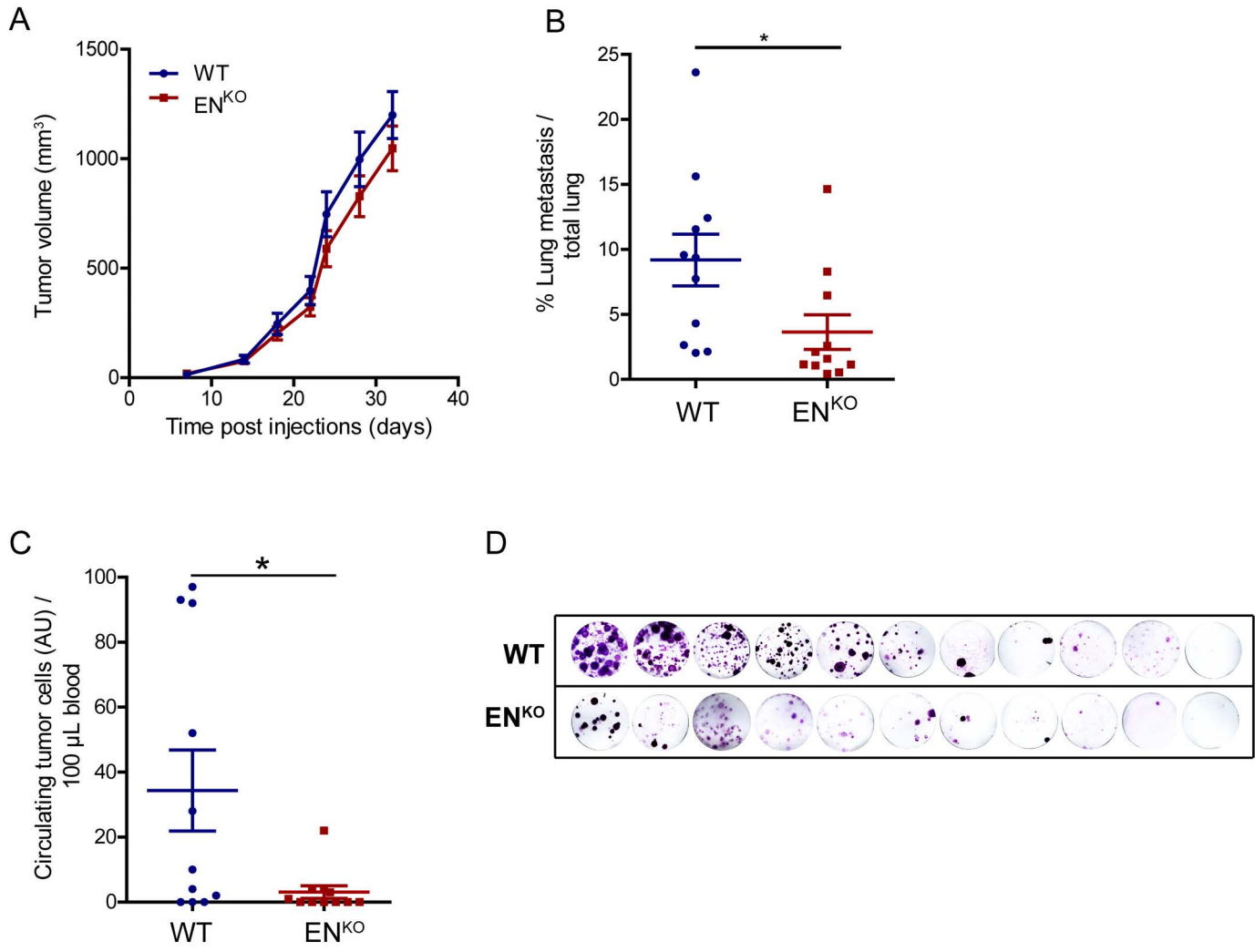
A, Comparison of endosialin (*CD248*) expression in 6 matched cases of microdissected breast tumor stroma and normal adjacent stroma (34). ***, $P=0.0003$, Two-tailed paired *t*-test. B, Human breast cancer samples stained for endosialin using B1/35 (0.6mm invasive breast cancer cores) or FB5 (whole invasive ductal carcinoma samples) antibody. Images illustrate negative, weak or strong endosialin expression in tumor stroma. Arrowheads indicate endosialin positive pericytes and myofibroblasts. Scale bar, 100 μ m. C, Quantification of stromal endosialin protein in invasive ductal carcinoma samples correlated to the lymph node metastasis status at the time of primary tumor removal and the distant metastasis status ~10 years after primary tumor removal. 47 patient samples analyzed. 8 patients, no metastasis; 19 patients, low metastatic potential (pN1a, 1-3 lymph nodes show tumors of 0.2cm size; 6 patients developed distant metastasis after primary tumor and lymph node removal); 12 patients, high metastatic potential (pN>1a, 4-10 lymph nodes show tumors of 0.2cm size; 5 patients developed distant metastasis after primary tumor and lymph node removal); 19 patients, distant metastasis (M1) to lung, brain, liver and bone. *, $P<0.05$, **, $P<0.01$. Two-tailed paired *t*-test. D, qPCR quantification (n=43) showing relative *CD248* mRNA levels in primary tumor samples from patients with no metastasis (n=9), low metastatic potential (n=9, pN1a), high metastatic potential (n=8, pN>1a) and distant metastasis (n=17, M1). *, $P<0.05$. Two-tailed paired *t*-test. E, Kaplan-Meier curves of recurrence-free survival assessed by the Finak et al. (34) dataset. $P=0.0474$, log-rank Mantel-Cox. F, Kaplan-Meier curves of distant metastasis-free survival assessed using publicly available data from Gyorffy et al. (35) (n=334 lymph node positive breast cancer samples). $P=0.035$, log-rank Mantel-Cox.

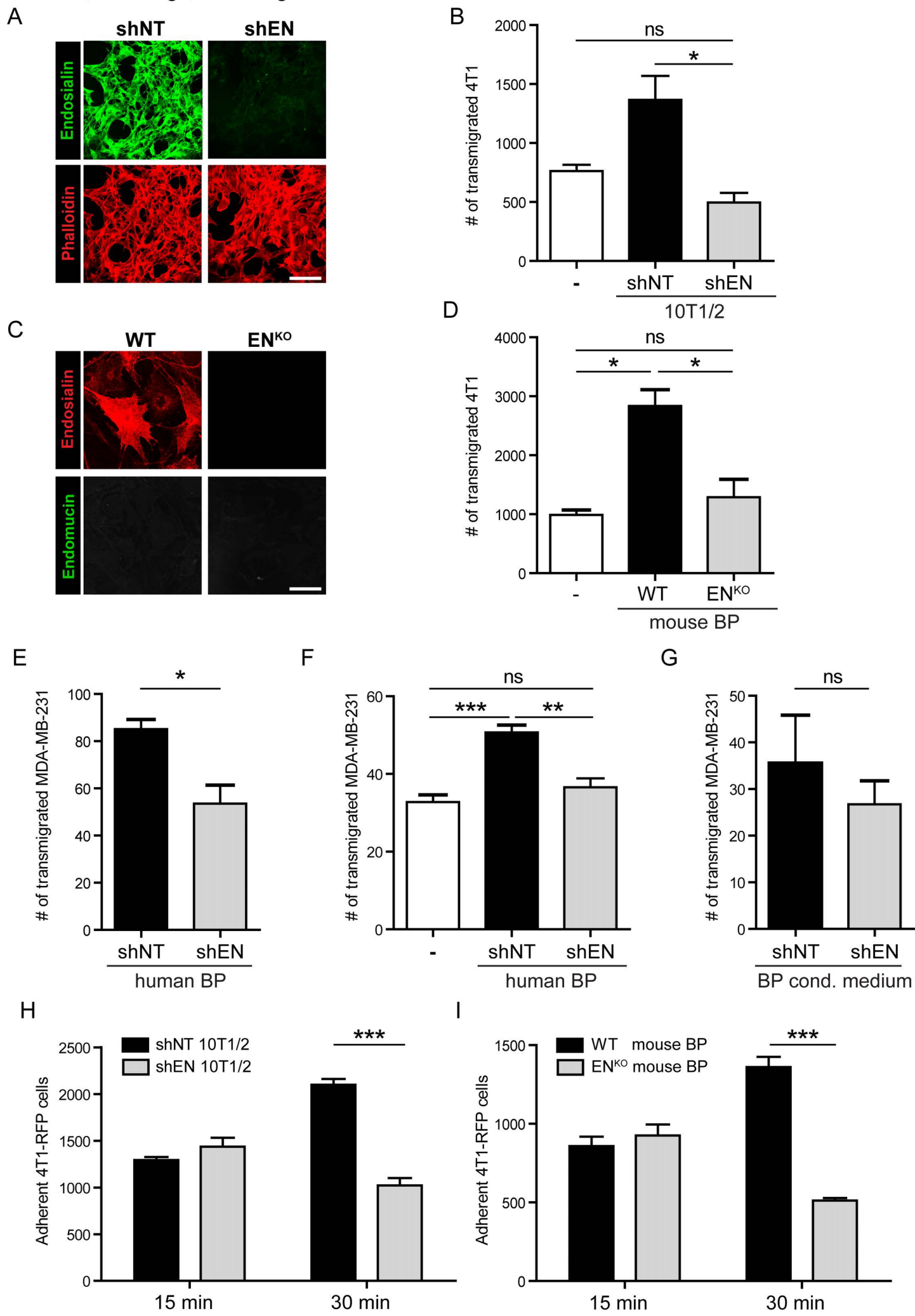












C. Viski*, C.König*, et al. Figure 7

